Immortalization of Primary Endothelial Cells by the K1 Protein of Kaposi's Sarcoma–Associated Herpesvirus

Ling Wang, Dirk P. Dittmer, Christine C. Tomlinson, Farnaz D. Fakhari, and Blossom Damania

Department of Microbiology and Immunology and Lineberger Comprehensive Cancer Center, University of North Carolina at Chapel Hill, Chapel Hill, North Carolina

Abstract

Kaposi's sarcoma–associated herpesvirus (KSHV) is linked to three different human cancers: Kaposi's sarcoma, primary effusion lymphoma, and multicentric Castleman's disease. The Kaposi's sarcoma lesion expresses high levels of angiogenic factors and is comprised of a mixed cell population, including endothelial cells that are infected with KSHV. We find that the KSHV K1 protein is expressed in Kaposi's sarcoma lesions and can immortalize and extend the life span of primary human umbilical vein endothelial cells in culture. Vascular endothelial growth factor (VEGF) is critical for the survival of endothelial cells, and we show that expression of K1 in endothelial cells resulted in increased levels of secreted VEGF and the activation of key signaling pathways, including the VEGF/VEGF receptor and the phosphatidylinositol-3′-OH-kinase (PI3K) pathway. The SH2 binding motifs present in the cytoplasmic tail of K1 were critical for K1's ability to activate these pathways. Activation of PI3K by K1 results in activation of Akt kinase and mammalian target of rapamycin and inactivation of the proapoptotic proteins FKHR, glycogen synthase kinase-3, and Bad, which are events indicative of cell survival. Because activation of the PI3K pathway is critical for transformation of many human cells, we suggest that PI3K activation by K1 is involved in endothelial cell immortalization and contributes to KSHV-associated tumorigenesis. We also report that K1 enhances angiogenesis *in vivo* and increases tumor vasculature and tumor size. (Cancer Res 2006; 66(7): 3658-66)

Introduction

Kaposi's sarcoma–associated herpesvirus (KSHV/HHV8) is a gammaherpesvirus that was first identified in Kaposi's sarcoma biopsies (1). KSHV is common to all epidemiologic forms of Kaposi's sarcoma, and its viral DNA is present in AIDS-associated Kaposi's sarcoma and in the vast majority of classic Mediterranean Kaposi's sarcoma (2, 3). KSHV has also been associated with B lymphoproliferative diseases, such as primary effusion lymphoma (PEL) and multicentric Castleman's disease (MCD; refs. 4, 5).

Kaposi's sarcoma is an angioproliferative disease, and the Kaposi's sarcoma lesion is comprised of proliferating fibroblasts, smooth muscle cells, infiltrating inflammatory cells, and activated endothelial cells. The endothelial cells are infected with KSHV and are thought to be the principal tumor cell in Kaposi's sarcoma lesions (6). Vascular endothelial growth factor (VEGF) is an important angiogenic growth factor that is expressed in Kaposi's sarcoma lesions and can induce endothelial cell growth and angiogenesis (7).

In Kaposi's sarcoma lesions, KSHV is present in every endothelial cell at 10 to 20 copies of the viral episome per cell (6, 8). Most tumor cells are latently infected, but low percentages of KSHV-infected cells undergo lytic reactivation (8). These observations led to the development of the paracrine hypothesis for Kaposi's sarcoma pathogenesis, in which KSHV induces a growth factor–rich microenvironment that supports continued proliferation of KSHV-infected cells, as well as neighboring, uninfected cells. This paracrine mechanism to induce growth proliferation also extends to other viruses, such as SV40, where large T antigen expression in human mesothelioma cells has been shown to correlate with the synthesis and release of hepatocyte growth factor (HGF) into the surrounding media, thereby activating the HGF receptors on surrounding cells (9).

The K1 protein of KSHV is a transmembrane glycoprotein encoded by the first open reading frame of the KSHV genome. It is located in an equivalent position to that of the saimiri transformation–associated protein of herpesvirus saimiri and the *R1* gene of rhesus monkey rhadinovirus (10). Expression of K1 in rodent fibroblasts produces morphologic changes and foci formation, characteristics indicative of cell transformation (11), and K1 transgenic mice develop sarcomas and plasmablastic lymphomas and display constitutive activation of nuclear factor-κB, Oct-2, and Lyn (12). It is important to note that these studies were done in murine/rodent cells, which are much more susceptible to neoplastic events than human cells because they spontaneously immortalize in cell culture (13).

The K1 cytoplasmic tail contains two SH2 binding motifs that together constitute an immunoreceptor tyrosine-based activation motif (ITAM). ITAMs are found in a variety of immune receptor complexes and play central roles in signal transduction events, leading to cell proliferation, differentiation, and death. K1 is capable of inducing multiple signaling events in B cells (14, 15). Our lab has previously shown that K1 can elicit matrix metalloproteinase-9 and VEGF production in endothelial cells (16), two factors implicated in angiogenesis and cell invasion. K1 is highly expressed during the viral lytic cycle, and K1 expression in infected cells may therefore be able to activate surrounding uninfected endothelial cells through the up-regulation of angiogenic growth factors in a paracrine fashion. Thus, K1 is an attractive candidate for playing a direct role in KSHV pathogenesis.

VEGF's biological effects are mediated via cell surface–expressed receptors, VEGFR-1 (Flt-1), VEGFR-2 (KDR or Flk-1 expressed predominantly in endothelial cells), and VEGFR-3 (Flt-4; ref. 17). Binding of VEGF to its receptors triggers autophosphorylation of the tyrosines in the VEGFR cytoplasmic tail. The phosphorylated

Note: B. Damania is a Leukemia and Lymphoma Society Scholar.

Requests for reprints: Blossom Damania, Lineberger Comprehensive Cancer Center, University of North Carolina, CB #7295, Chapel Hill, NC 27599. Phone: 919-843-6011; Fax: 425-930-1087; E-mail: damania@med.unc.edu.

doi:10.1158/0008-5472.CAN-05-3680

tyrosines then bind to various signaling molecules, resulting in the activation of the phosphatidylinositol-3 kinase (PI3K) and mitogen-activated protein kinase pathways (18).

The PI3K/Akt signaling pathway is involved in cell growth and survival (19). PI3Ks are heterodimers composed of a catalytic subunit (p110) and an adaptor/regulatory subunit (p85), which are activated by receptors with protein tyrosine kinase activity (RPTK; ref. 19). Upon RPTK activation, PI3K associates with the receptor through one or two SH2 domains in p85, which results in allosteric activation of p110 (20). PI3K activation leads to phosphorylation of the lipid membrane–associated moiety phosphatidylinositol 4,5-bisophosphate (PIP2), which yields second messenger phosphatidylinositol 3,4,5-triphosphate (PIP3). Akt specially binds PIP3 and is subsequently phosphorylated at Thr^{308} and Ser^{473} by the 3-phosphoinositide-dependent protein kinase 1 (PDK1) and PDK2 (21, 22). The negative regulator of this pathway is the phosphatase and tensin homologue (PTEN; ref. 23).

Akt is a critical regulator of PI3K-mediated cell survival (24–26). Activated Akt promotes cell survival mechanisms by directly phosphorylating and inactivating apoptotic factors, such as Bad and the forkhead transcription factors (27, 28). Akt also regulates glycogen synthesis through the phosphorylation and inactivation of glycogen synthase kinase-3 (GSK-3β; ref. 29). Akt enhances protein synthesis through increasing the phosphorylation of mammalian target of rapamycin (mTOR; ref. 30).

It is currently well established that tumor progression is angiogenesis dependent, that many tumor cell lines secrete VEGF *in vitro*, and that VEGF mRNA levels are increased in most human tumors. Here, we report that K1 can immortalize primary human umbilical vein endothelial cells (HUVEC) and activate both the VEGF/VEGFR-2 and the PI3K/Akt signaling pathway in endothelial cells. We also found that K1 expression in C33A epithelial cells contributes to increased angiogenesis *in vivo* because mice injected with these cells showed increased tumor size and tumor vascularity.

Materials and Methods

Plasmids. The retroviral vector pLXCN/GFP was kindly provided by Dr. Enrique A. Mesri (31). Using the pLXCN/GFP vector, we constructed pLXCN/Flag-K1 and pLXCN/Flag-$K1_{SH2-}$.

Retroviral production. 293T human kidney epithelial cells (American Type Culture Collection, Rockville, MD) were cultured in DMEM (Sigma, St. Louis, MO) with 10% fetal bovine serum (FBS), penicillin, and streptomycin and maintained at 37°C in a 5% CO_2 environment. Cells were grown in 100-mm dishes and were cotransfected with 7 μg pVSV-G and pGAG-pol and either 7 μg pLXCN/GFP, pLXCN/K1, or pLXCN/$K1_{SH2-}$ using CalPhos Mammalian Transfection kit (BD Biosciences, Bedford, MA). Supernatants containing green fluorescent protein (GFP), Flag-K1, and Flag-$K1_{SH2-}$ retroviruses were harvested 48 hours later. Virus was pelleted using ultracentrifugation at 25,000 rpm for 3 hours.

Retroviral transduction and stable cell lines. Immortalized HUVECs-hTERT (16) and primary HUVECs (Clonetics, San Diego, CA) passage 6 were cultured in endothelial growth medium (EGM-2, Clonetics) with 10% FBS. For retroviral infections, cells were plated in 100-mm dishes and infected with GFP or K1 retroviruses in the presence of polybrene (8 μg/mL). The cells were selected in neomycin (G418, Invitrogen, San Diego, CA; 0.1 mg/mL for HUVECs and 0.6 mg/mL for C33A cells) for 2 weeks.

Analysis of VEGFR-2/Flk-1 phosphorylation. Cell lysates containing equal amounts of protein were incubated with monoclonal anti-Flk-1 antibody (Santa Cruz Biotechnology, Santa Cruz, CA) and protein A/G PLUS-agarose (Santa Cruz Biotechnology). The precipitates were washed thrice with lysis buffer and then subjected to SDS-PAGE and transferred to nitrocellulose membrane. Western blots were done with monoclonal anti-phosphotyrosine horseradish peroxidase (HRP) conjugate (1:1,000 dilution; Upstate, Lake Placid, NY). Expression of VEGFR-2 was determined by Western blot with anti-Flk-1 antibody (Santa Cruz Biotechnology).

Analysis of PI3K/Akt activation. The HUVEC-GFP, HUVEC-K1, and HUVEC-$K1_{SH2-}$ cells were serum starved for 48 hours with endothelial basic medium (EBM-2, Clonetics). The cells were washed with ice-cold PBS containing 1 mmol/L Na_3VO_4 and protease inhibitor cocktail (Roche, Mannheim, Germany) and then lysed in Triton/NP40 lysis buffer.

Western blots were done with the indicated antibodies, which were purchased from Cell Signaling Technology (Beverly, MA). For the inhibition study, LY294002 (Sigma) was used to inhibit PI3K activation. The cells were serum starved for 48 hours, and 16 hours before harvest, the cells were treated with 10 μmol/L LY294002 or methanol (vehicle). The cell lysates were harvested, and Western blots were done to detect the phosphorylation of Akt.

Cell survival assays. Primary HUVECs-GFP and HUVECs-K1 (1×10^5; passage 8) were plated in each well of a six-well plate and cultured in G418-containing media at 37°C. Cells were trypsinized and counted using a hemocytometer and trypan blue several times a week.

Telomerase detection assay. To detect telomerase activity, 1×10^5 primary HUVECs-GFP and HUVECs-K1 were harvested and resuspended with CHAPS lysis buffer. The cell lysates were used for PCR, and then the PCR products were loaded and run on a polyacrylamide gel according to the manufacturer's protocol for the TRAPEZE Telomerase detection kit (Chemicon, Temecula, CA).

Tumorigenicity in mice. For the C33A cell lines, six groups of five mice each (total = 30) were inoculated respectively with 1×10^5 C33A-GFP cells (clones 2, 5, and 8) and C33A-K1 (clones 8, 9, and 16) per mouse. Cells were counted, and indicated cell doses were diluted in 200 μL growth factor–depleted Matrigel (BD Biosciences). Cells were injected s.c. into the right flank into C.B.-17 severe combined immunodeficient mice (The Jackson Laboratory, Bar Harbor, MN). Tumor size was measured with a caliper. The tumors were excised and fixed in formalin.

Immunohistochemistry. Tumors from C33A-GFP and C33A-K1 injected mice were formalin fixed and paraffin embedded, and 8-μm-thick sections were prepared using a microtome. Sections were deparaffinized with Histochoice clearing reagent (Sigma) and hydrated with water before microwave treatment in 1 mmol/L EDTA (pH 8) for 15 minutes for antigen retrieval and then blocked with blocking solution (10% normal horse serum, 5% bovine serum albumin, and 0.3% Triton X-100 in PBS). Sections were incubated with the indicated antibodies either overnight at 4°C or for 1 hour at room temperature. Secondary antibody was provided in the Vectastain Avidin-Biotin Complex Systems kit, and staining was done with the VECTOR NovaRED Substrate kit (Vector Laboratories, Burlingame, CA) and hematoxylin. Immunohistochemistry was also done to detect K1 expression. Kaposi's sarcoma tumors sections were incubated with anti-K1 polyclonal antibody (1:100) for 1 hour at room temperature followed by secondary antibody staining as described above.

Results

K1 prolongs the life span of primary HUVECs. Primary HUVECs normally senesce after a limited number of cell doublings in culture. We did a cell survival assay to determine whether the KSHV K1 viral protein could extend the life span of primary HUVECs. We infected primary HUVECs with retroviruses expressing either K1 or GFP and selected the cells in neomycin containing media to ensure continued expression of GFP or K1. We plated 1×10^5 cells of primary HUVEC-GFP and HUVEC-K1 into each well of a six-well plate in triplicate. When confluent, live cells were trypsinized and counted using a hemocytometer and trypan blue staining, after which 1×10^5 cells per well were replated in a six-well dish and grown at 37°C. This procedure was repeated over a period of several months. Thus far, we have found that the primary HUVEC-GFP cell line could be passaged 32 times before undergoing senescence,

whereas the primary HUVEC-K1 cells have now been passaged 55 times and are currently still growing. Between passage 8 and passage 15, the primary HUVEC-GFP and HUVEC-K1 displayed very similar growth rates, but after passage 15, the HUVEC-K1 cells grew faster than the HUVEC-GFP (Fig. 1*A*). After passage 32, the primary HUVEC-GFP cells went into terminal replicative arrest and stopped growing, and their morphology appeared senescent, ramose, and flattened. However, the primary HUVEC-K1 cells kept growing and maintained normal endothelial cell morphology. Cell immortalization is the consequence of overriding the normal cellular mechanism of senescence and apoptosis, and telomere maintenance is necessary for cell proliferation (32). Telomere stability depends on activation of telomerase (Tert), an enzyme that synthesizes telomere repeat sequences to replace those that are lost during DNA replication. However, in other cell lines and cancers, telomere length is maintained by an alternative lengthening of telomeres (ALT) mechanism (33, 34). To investigate the molecular mechanism by which K1 extends the life span of primary HUVECs, we tested telomerase (hTert) activity in these cells using a telomerase detection assay (Fig. 1*B*). Cell lysates from the HUVEC-K1 and HUVEC-GFP lines were incubated with telomere-specific primers and primers for an internal template amplification sequence control. The extracts were either untreated or heat treated before being subjected to PCR amplification. The heat-treated extracts served as a negative control for telomerase activity. The PCR products were loaded and run on a polyacrylamide gel. Positive extracts yield a 36-bp internal product and a ladder of products with 6-base increments starting at 50 nucleotides. As shown in Fig. 1*B*, no increased telomerase activity was detected in the primary HUVEC-K1 cell line compared with the vector control. These results suggest that telomere maintenance in primary HUVECs expressing K1 is probably carried out by an ALT mechanism (33, 34).

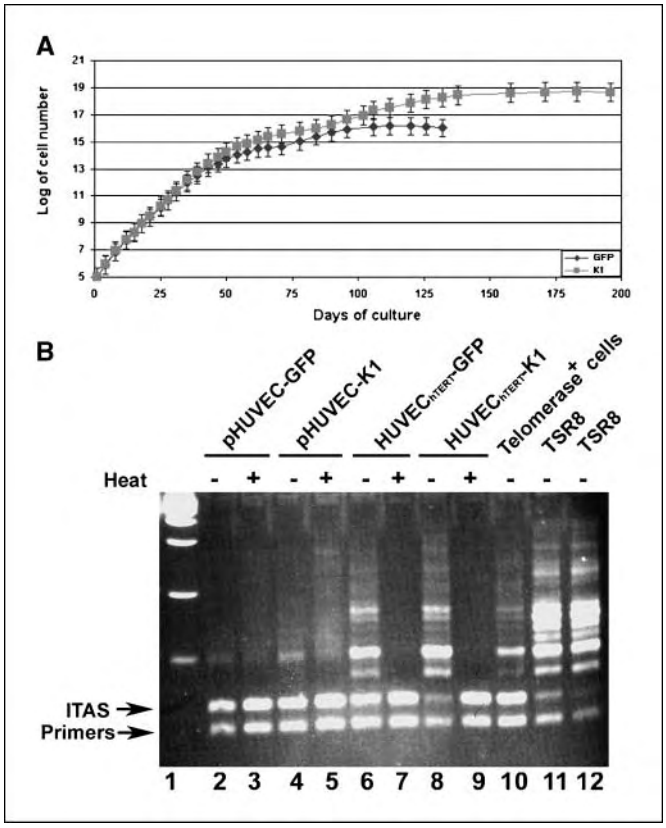

Figure 1. KSHV K1 can immortalize primary HUVECs. *A,* primary HUVECs (passage 6) were infected with retroviruses expressing K1 or GFP and cultured in G418-containing media. Cells were trypsinized and counted using a hemocytometer and trypan blue staining. The number (log) of live cells is plotted over days in culture. After passage 32, the primary HUVEC-GFP cells went into terminal replicative arrest, whereas the primary HUVEC-K1 cells kept growing and maintained normal endothelial cell morphology and behavior. *B,* telomerase activity in primary HUVEC-K1 and HUVEC-GFP cell lines. Primary HUVEC-GFP (*pHUVEC-GFP*; 1×10^5) and primary HUVEC-K1 (*pHUVEC-K1*) were harvested in lysis buffer. As a control, hTert-immortalized HUVECs expressing GFP (HUVEC$_{hTERT}$-GFP) or K1 (HUVEC$_{hTERT}$-K1) were also used. Cell lysates were amplified with telomere-specific primers and primers for an internal template amplification sequence (*ITAS*) control. *Lane 1,* DNA marker; *lanes 2-5,* telomerase activity in untreated or heat-treated pHUVEC-GFP and pHUVEC-K1 cells, respectively; *lanes 6-9,* telomerase activity in untreated or heat-treated hTert-immortalized HUVEC-GFP or HUVEC-K1 cells, respectively; *lane 10,* positive control using cell lysates containing telomerase activity; *lanes 11* and *12,* additional positive controls for the amplification of telomeric repeats.

We next investigated whether the immortalized HUVEC-K1 cells were transformed. Early-passage HUVEC-K1 and HUVEC-GFP cells were s.c. injected into two groups of $n = 5$ nude mice at a concentration of 5×10^6 per mouse in Matrigel. In the presence of Matrigel, transformed cells typically form tumors within 21 days if $\geq 10^6$ cells are inoculated (35). After 4 weeks, we observed no tumor growth in either the mice injected with HUVEC-GFP or HUVEC-K1 cells (data not shown), suggesting that although the HUVEC-K1 cells were immortalized, they were not transformed.

K1 induces phosphorylation of VEGFR-2/Flk1. We next tested the hypothesis that K1's ability to immortalize primary endothelial cells was dependent on growth factor signaling for endothelial cell proliferation. We had previously established hTert-immortalized HUVECs (16). We transduced the immortalized HUVECs with either K1- or GFP-expressing retroviruses as described in Materials and Methods. Infected cells were selected with G418 for several weeks to generate stable HUVEC-GFP and HUVEC-K1 cell lines.

We first tested the ability of the K1-expressing HUVEC cells to increase secretion of VEGF. Figure 2*A* shows a 4-fold increase in the levels of secreted VEGF protein in these cells compared with the vector control. We next determined whether VEGFR-2, the predominant VEGFR on endothelial cells, was activated in the K1-expressing HUVECs. Briefly, the HUVEC-GFP and HUVEC-K1 cells were treated with serum-free media 48 hours before cell harvest. Equal micrograms of HUVEC-K1 and HUVEC-GFP cell lysates were used to perform an immunoprecipitation with an anti-Flk-1 (VEGFR-2) antibody overnight. The immunoprecipitates were subjected to Western blot analysis with an anti-phosphotyrosine-HRP–conjugated antibody. As can be seen in Fig. 2*B* (*top*), K1 expression dramatically induced the tyrosine phosphorylation of VEGFR-2 in endothelial cells, suggesting that VEGFR-2 is activated in K1 cells compared to the GFP control. However, K1 expression had no significant effect on the total protein level of VEGFR-2 in endothelial cells (Fig. 2*B, middle*). VEGFR activation is likely a consequence of K1's ability to up-regulate VEGF expression and secretion in these cells.

K1 Activates the PI3K/Akt signaling pathway. Activation of the VEGF/VEGFR signaling pathway has previously been shown to lead to phosphorylation and activation of p85, the adaptor/regulatory subunit of PI3K (36). Because we observed that K1 can activate VEGFR-2, we were interested in determining whether the PI3K/Akt signaling pathway was also activated in endothelial cells. The HUVEC-GFP and HUVEC-K1 cell lines were serum starved for 48 hours. Equivalent amounts of lysate were loaded on SDS-PAGE and subjected to Western blot analysis with antibodies directed against components of the PI3K/Akt pathways. K1 expression

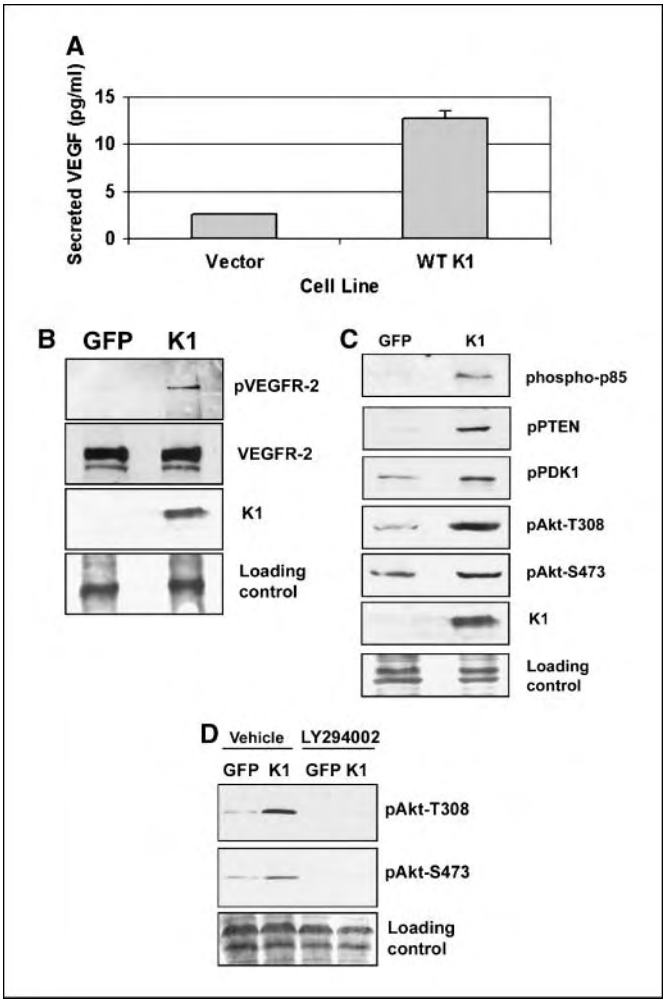

Figure 2. K1 increases VEGF secretion from endothelial cells and activates the VEGF/VEGFR and PI3K/Akt signaling pathways. *A,* conditioned media were collected from HUVECs expressing either vector control or wild-type K1, and a VEGF ELISA was done. The quantity of secreted VEGF shown represents a 1:50 dilution of the HUVEC cell supernatant. Wild-type K1 protein induced the secretion of VEGF from endothelial cells ~4-fold higher than vector alone. *B,* K1 expression in endothelial cells activates the VEGF/VEGFR signaling pathway. HUVEC-GFP or HUVEC-K1 stable cells were lysed, and an immunoprecipitation was done using an anti VEGFR-2 antibody. Immunoprecipitates were subjected to SDS-PAGE followed by Western blot against phospho-tyrosine. VEGFR-2 was phosphorylated in K1-expressing HUVECs but not in the GFP-expressing cells (*top*), whereas the levels of total VEGFR-2 protein remained equal. Western blots were also done for K1 expression and loading controls. *C,* stable HUVECs expressing either GFP or K1 were harvested. Equal micrograms of lysate were subjected to SDS-PAGE, and Western blot analyses were done for phospho-p85, phospho-PTEN (*pPTEN*), phospho-PDK1 (*pPDK1*), and phospho-Akt at Thr^{308} (*pAkt-T308*) and Ser^{473} (*pAkt-S473*). K1-expressing HUVECs showed increased levels of phosphorylation of p85, PDK1, and Akt kinases and the PTEN phosphatase. *D,* K1's activation of Akt kinase is PI3K specific. HUVEC-GFP or HUVEC-K1 cells were serum starved for 48 hours followed by treatment with 10 μmol/L LY294002 16 hours before harvest. Cell lysates were subjected to Western blotting with anti-phospho-Akt antibodies as described above.

resulted in the phosphorylation of the p85 subunit of PI3K (Fig. 2*C*), indicative of its activation. To analyze the functional consequences of p85 activation, additional Western blots were done with antibodies against phospho-PTEN (Ser^{380}), phospho-PDK1 (Ser^{241}), phospho-Akt (Thr^{308}), and phospho-Akt (Ser^{473}). K1 expression increased both the phosphorylation of the negative regulatory phosphatase (PTEN) at Ser^{380}, which corresponds to its inactivation, and the phosphorylation of the PDK1 kinase at Ser^{241}, which corresponds to its activation (Fig. 2*C*). Thus, the net effect of K1 expression in endothelial cells is activation of the PI3K pathway.

Congruent with these results, K1-expressing HUVECs showed an increase in the phosphorylation of Akt at Ser^{473} and Thr^{308} (Fig. 2*C*), events that indicate a fully activated kinase. To determine if Akt activation was PI3K dependent, we treated the GFP- and K1-expressing HUVECs with the PI3K inhibitor LY290042. K1's effect on Akt activation and phosphorylation was PI3K specific because treatment of these cells with LY290042 significantly inhibited Akt phosphorylation and activation at both Ser^{473} and Thr^{308} (Fig. 2*D*).

To detect K1's effects on the downstream targets of Akt, we performed Western blot analyses on extracts from HUVECs expresxsing either K1 or GFP. We observed that all the downstream targets of Akt we tested, including GSK3β, FKHRL1, FKHR, Bad, and mTOR, were significantly phosphorylated in HUVECs expressing K1 but not GFP (Fig. 3*A*). Phosphorylation of GSK3β, FKHRL1, FKHR, and Bad have been shown to correspond to their inactivation (27, 29, 37).

K1 expression also increased the phosphorylation of mTOR by Akt, resulting in its activation (38). Activated mTOR up-regulates both ribosomal biosynthesis and translation of mRNAs that are essential for G_1-S phase progression. In summary, we observed that expression of K1 in endothelial cells resulted in the inactivation of proapoptotic proteins and the activation of mTOR, a kinase involved in protein synthesis.

SH2 binding motifs of K1 are necessary for activation of the PI3K/Akt signaling pathway. Although the cytoplasmic tail of K1 is a highly variable domain among different KSHV viral isolates throughout the world, the SH2 binding motifs present in the cytoplasmic tail are always conserved (39). We mutated the two SH2 binding motifs in K1 by replacing the tyrosine residues with phenylalanine residues and tested whether this mutation ($K1_{SH2-}$) abolished PI3K/Akt signaling pathway. We constructed a second set of wild-type (WT) K1, GFP, and $K1_{SH2-}$ mutant expressing endothelial cell lines and analyzed the components of the PI3K/Akt signaling pathway. As shown in Fig. 3*B*, expression of the mutant $K1_{SH2-}$ protein could not induce phosphorylation and activation of Akt kinase compared with WT K1. Consequently, downstream targets of Akt, including GSK3β, FKHR, Bad, and mTOR, did not display increased phosphorylation in the $K1_{SH2}$-expressing cells compared with WT K1 (Fig. 3*C*). These data indicate that the SH2 binding motifs of K1 are necessary for activation of the PI3K/Akt pathway and phosphorylation of its downstream targets in endothelial cells.

K1 expression in epithelial cells results in increased tumor size and increased vasculature *in vivo*. We have previously shown that K1 can induce the expression and secretion of VEGF from epithelial cells (16). To determine whether epithelial cells expressing K1 exhibit increased tumorigenic potential in mice, we used the human C33A cervical carcinoma cell line, which is human papillomavirus–negative. C33A cells by themselves are tumorigenic in nude mice (40), and we wanted to determine whether the introduction of K1 in these cells could enhance the tumorigenicity and/or angiogenic nature of these tumors.

K1 and GFP-expressing stable C33A cell lines were made by retroviral infection. Cells were selected with neomycin over several weeks, and three different clones each of the C33A-K1 and C33A-GFP stable cell lines were established. Expression of GFP was analyzed by microscopy, and expression of K1 in each clone was determined by Western blot (Fig. 4*A*).

Six groups of five nude mice each were injected with individual clones of C33A-GFP and C33A-K1 cells using a suboptimal dose of

only 1×10^5 per mouse, and the mice were monitored for 3 to 4 weeks. At this dose, ≤50% of mice injected with C33A-GFP cells developed tumors by 21 days, whereas 100% of mice injected with C33A-K1 cells developed palpable tumors. The cumulative mean tumor-free survival time was shorter in mice injected with the C33A-K1 cells compared with mice injected with C33A-GFP (Fig. 4*B*). Consistent with Institutional Animal Care and Use Committee requirements, the experiment was terminated when the tumor diameter exceeded 5 mm or the statistical difference between groups amounted to $P \leq 0.05$. This result was significant to $P \leq 0.02$ by log-rank test. The average sizes of tumors that developed in mice injected with C33A-K1 were bigger than those injected with C33A-GFP throughout the observational period (Fig. 4*C*). The tumor size differences between the C33A-GFP and

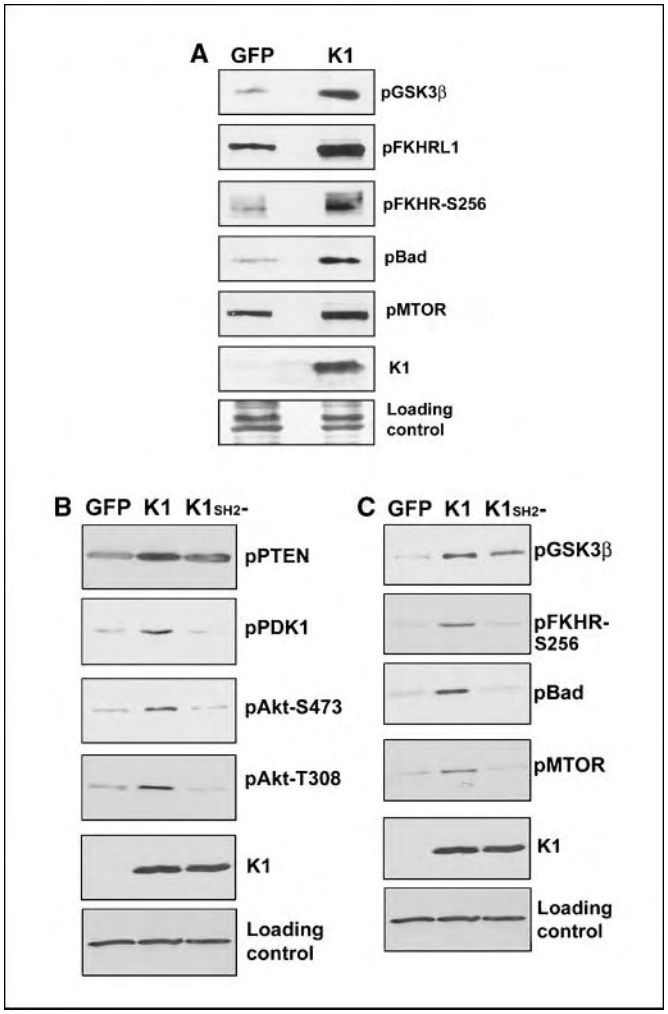

Figure 3. K1-expressing endothelial cells show increased phosphorylation of all analyzed downstream targets of PI3K/Akt. *A,* extracts from the HUVEC-GFP and HUVEC-K1 stable cells were subjected to Western blot analyses for the downstream targets of the PI3K/Akt pathway as indicated. K1-expressing endothelial cells showed increased phosphorylation of GSK3β (*pGSK3β*), FKHRL1 (*pFKHRL1*), FKHR (*pFKHR*), Bad (*pBad*), and mTOR (*pMTOR*). *B,* HUVECs stably expressing GFP (HUVEC-GFP), wild-type K1 (HUVEC-K1), and K1 containing mutations in the SH2 binding motifs (HUVEC-$K1_{SH2-}$) were analyzed for activation of the PI3K/Akt pathway. We observed that wild-type K1 expressing HUVECs showed an increased amount of phospho-PDK1 (*pPDK1*) and phospho-Akt (pAKt) kinase compared with the GFP control, while the $K1_{SH2-}$ mutant failed to induce phosphorylation and activation of Akt kinase. *C,* phosphorylation of the downstream targets of Akt were increased in wild-type K1 expressing HUVECs but not in the K1 mutant expressing cells. We tested the phosphorylation and activation status of members of the PI3K/Akt pathway in WT HUVEC-K1, HUVEC-$K1_{SH2-}$, and HUVEC-GFP cells. PTEN is the negative regulator of PI3K, and its phosphorylation is concordant with its inactivation. Phosphorylation of PDK1 and Akt correlate with the activation of these kinases. Phosphorylation of the downstream targets of Akt kinase, GSK3β, FKHR, and Bad correlate with their inactivation, whereas phosphorylation of mTOR correlates with its activation.

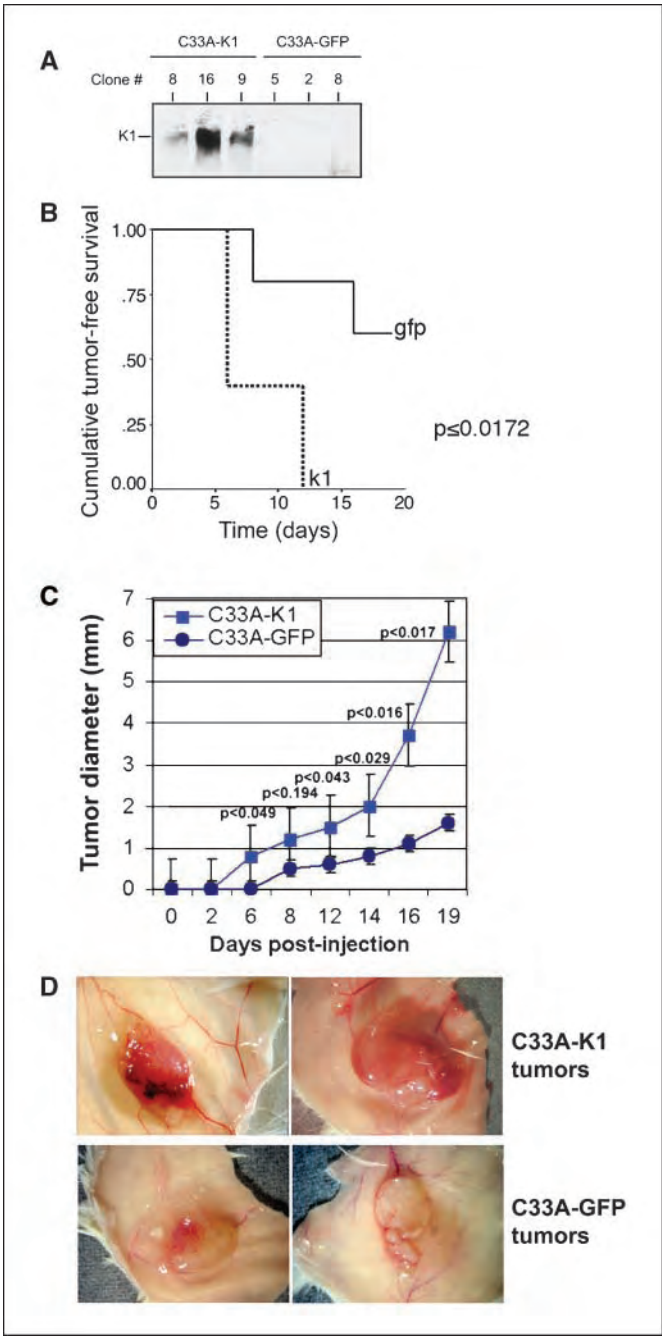

Figure 4. K1 increases tumor size and tumor angiogenesis *in vivo*. *A,* three C33A-K1 clones were analyzed for K1 expression by Western blot. *B,* Kaplan-Meier plot showing cumulative tumor-free survival of all the mice injected with 1×10^5 C33A-K1 or C33A-GFP cells per mouse. *C,* six groups of five mice each were s.c. injected with 1×10^5 C33A-K1 clones 8, 16, and 9 and C33A-GFP clones 5, 2, and 8. Tumor diameter was measured in two dimensions using calibrated calipers, and average tumor diameter (mm) is plotted over days after injection. *Points,* mean from five animals for each cell type; *bars,* SE. *D,* evaluation of the C33A-GFP and C33A-K1 tumors indicated that the C33A-K1 tumors were more angiogenic and more vascularized compared with the C33A-GFP tumors with more blood vessels developing around the C33A-K1 tumors.

C33A-K1 tumors were statistically significant by ANOVA with $P \leq 0.001$ considering all time points, and at days 16 and 19 with $P \leq 0.05$ using Mann-Whitney test ($n = 10$).

In a second experiment, we increased the dose using 1×10^6 C33A-GFP and C33A-K1 cells per s.c. injection in each mouse and observed similar results (data not shown). Upon gross examination (Fig. 4*D*), the C33A-K1 tumors seemed more angiogenic and vascularized compared with the C33A-GFP tumors, and more blood vessels had developed around the C33A-K1 tumors. Significance was $P \leq 0.02$ by t test for tumor weight ($n = 30$, six independent lines). Taken together, our results show that K1 expression enhances tumor vasculature, tumor size, and tumor weight *in vivo*.

We next determined if Akt was activated in the C33A-K1 tumors that developed in the mice. Immunohistochemistry was done using tissue sections from C33A-GFP and C33A-K1 tumors to detect expression of phospho-Akt (S473), Ki67 (proliferation marker), and K1 (Fig. 5). Ki67 is a prototypic cell cycle–related nuclear protein expressed by proliferating cells in all phases of the active cell cycle. As a proliferation marker, Ki67 expression was expressed in a higher proportion of cells in C33A-K1 tumors compared with C33A-GFP tumors (Fig. 5*A*), suggesting that the C33A-K1 tumor cells were actively proliferating. Immunohistochemistry of the tumor sections showed that Akt was phosphorylated in C33A-K1 tumors but not in the C33A-GFP tumors (Fig. 5*B*, *a* and *c* compared with *b* and *d*, respectively). Thus, in the tumor, as in the endothelial cells, overexpression of K1 results in Akt phosphorylation and activation of Akt-dependent survival signals. To verify that K1 was expressed in the C33A-K1 tumors, we used HRP-conjugated anti-FLAG antibody, because K1 was FLAG tagged. K1 was expressed in C33A-K1 tumors (Fig. 5*C*, *e* and *g*) but not in C33A-GFP tumors (Fig. 5*C*, *f* and *h*).

To evaluate tumor proliferation, we quantified Ki-67 staining. For each tumor section, three regions were selected, and within each region, the number of positive cells (Ki-67 index) was determined for five fields at ×400 magnification. This yielded a total of $n = 135$ data points. The differences in Ki-67 index between K1 and GFP tumors were significant to $P \leq 0.0001$ by nonparametric (Mann-Whitney) test statistic (Fig. 5*D*). Hence, there was a higher percentage of Ki67-positive cells in the C33A-K1 tumors compared with the C33A-GFP tumors (Fig. 5*D*). This explains why the C33A-K1 tumors were bigger than the C33A-GFP tumors.

K1 expression in Kaposi's sarcoma tumors. Previous data have shown that K1 transcripts have been detected in human Kaposi's sarcoma tissues (41) and Lee et al. detected K1 expression in PEL and MCD using a monoclonal K1 antibody (42). We used an anti-K1 polyclonal antibody to detect K1 expression in multiple Kaposi's sarcoma tumor sections. We obtained a Kaposi's sarcoma tissue microarray TA03-008 from the AIDS and Cancer Specimen Resource (ACSR). This array contains 170 × 0.6 mm cores from 55 HIV-positive Kaposi's sarcoma patients that represent historical submissions to the ACSR.

Interestingly, we found variable expression of K1 in Kaposi's sarcoma tumors. A few Kaposi's sarcoma tumors had no detectable K1 expression (Fig. 6*A*, *a*), many tumors displayed a high level of K1

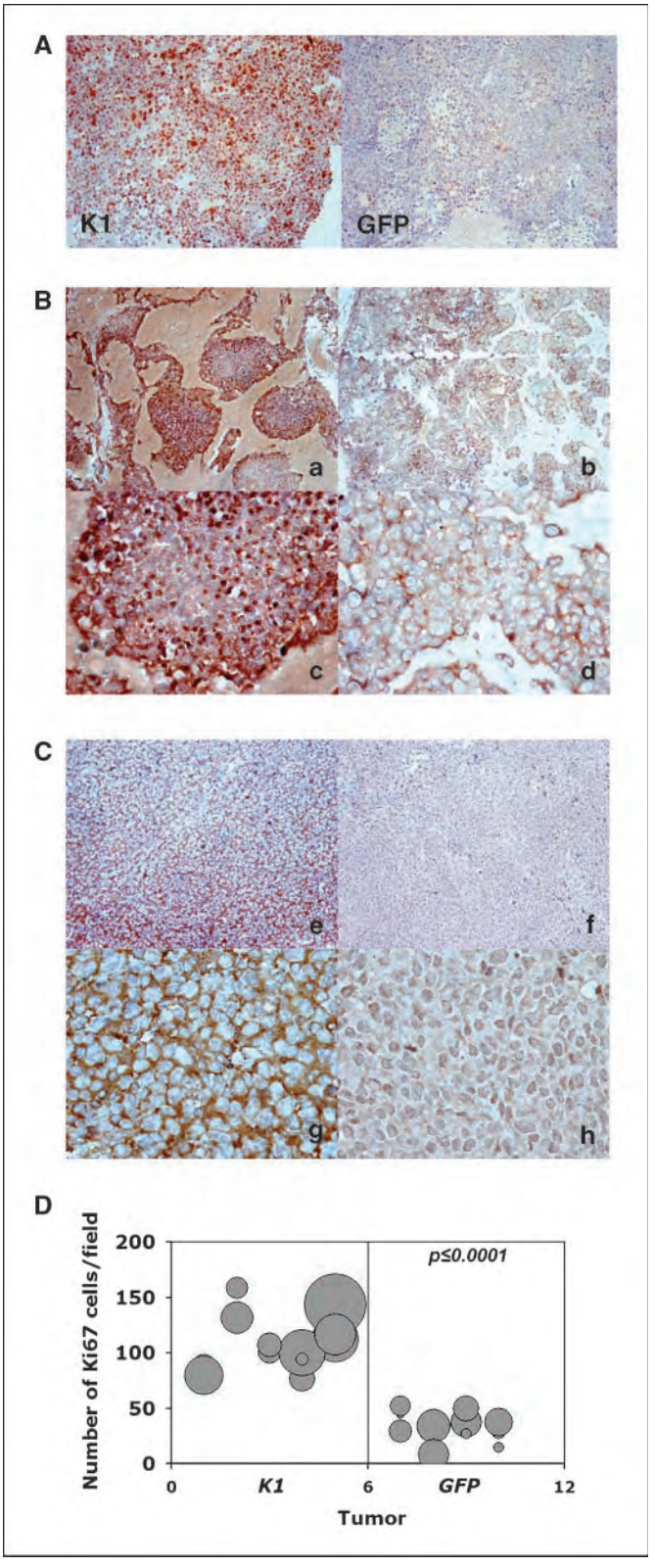

Figure 5. K1 increases cell proliferation and activates Akt *in vivo*. *A,* staining of the C33A-GFP and C33A-K1 tumors with anti-Ki67 antibody at ×100 magnification. *B,* staining of the C33A-GFP and C33A-K1 tumors with anti-phospho-Akt (S473) antibody. *a* and *c,* C33A-K1 tumors; *b* and *d,* C33A-GFP tumors. Magnification, ×40 (*a* and *b*) and ×400 (*c* and *d*). *C,* staining of the C33A-GFP and C33A-K1 tumors with anti-Flag antibody to detect K1 expression. *e* and *g,* C33A-K1 tumors; *f* and *h,* C33A-GFP tumors. Magnification, ×100 (*e* and *f*) and ×400 (*g* and *h*). *D,* mean number of $n = 5$ fields for three different regions (total of 15 fields) for each tumor at day 21 derived from either K1- or GFP-expressing C33A cells. The size of the circle correlates to the SE for each region.

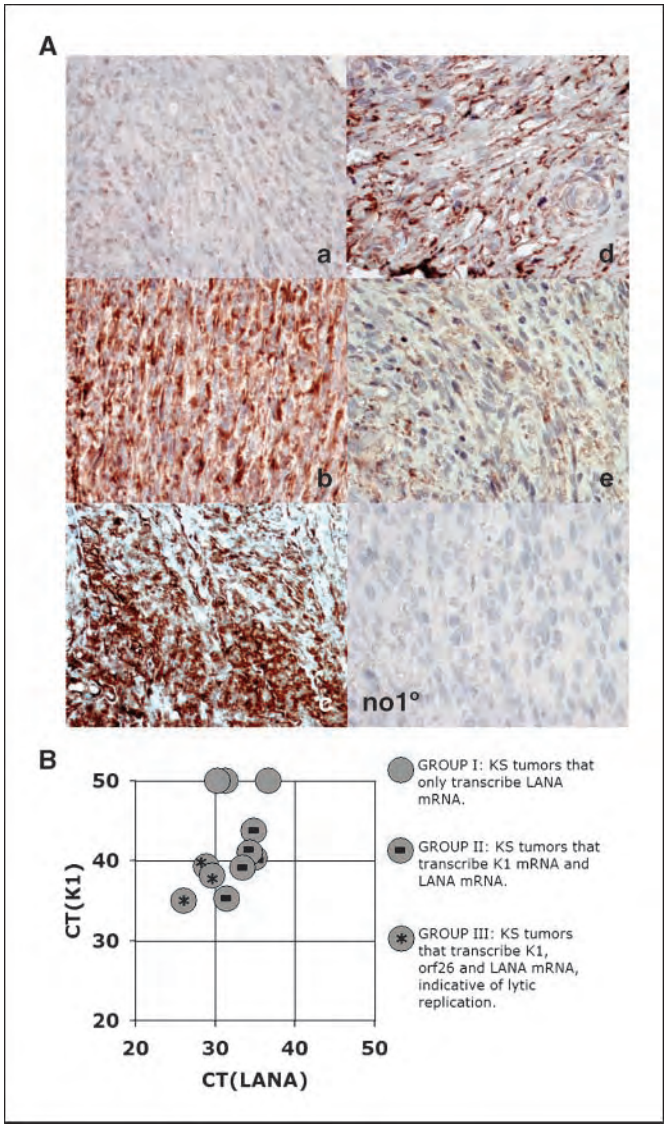

Figure 6. K1 protein and mRNA expression in Kaposi's sarcoma tumors. *A,* 400× magnification. *a-e,* staining of different Kaposi's sarcoma tumors in a Kaposi's sarcoma tissue array slide with anti-K1 polyclonal antibody. It is important to note that all the KS tumors were present on the same slide. *No1,* negative control in which the primary antibody was replaced with blocking solution to perform immunohistochemistry. *B*, detection of K1 mRNA in Kaposi sarcoma tumors; *horizontal axis,* relative levels (CT) of LANA mRNA; *vertical axis,* relative levels of K1 mRNA on a log 1.93 scale. Lower values correspond to higher abundance. CT = 50 represent the maximal cycle number in this experiment and limit of detection. There were three groups of KS tumors: Group I expressed LANA but no K1 mRNA; Group II expressed LANA and K1 mRNA but no Orf26 mRNA; and Group III expressed LANA, Orf26, and K1 mRNA, indicative of lytic replication.

expression (Fig. 6*A, b* and *c*), and other tumors had low K1 expression levels (Fig. 6*A, d* and *e*). It is important to note that all the Kaposi's sarcoma tumors were present on the same slide; hence, the variable expression levels of K1 in the different Kaposi's sarcoma tumors are authentic and not a result of background staining or artifact.

In addition, we also did real-time quantitative reverse transcription-PCR to detect the presence of K1 mRNA transcripts in 11 Kaposi's sarcoma lesions and correlated the levels of K1 mRNA to that of the KSHV latency–associated nuclear antigen (LANA) and a marker of late lytic replication, KSHV Orf26. Primers and procedures were previously published (43, 44). In our real-time QPCR array, CT values correspond to target mRNA levels on a log 1.93 scale. Lower CT values correspond to higher mRNA levels. We plotted the unmanipulated CT values for K1 against the CT values for LANA (Fig. 6*B*). Because LANA is transcribed in every KSHV-infected Kaposi's sarcoma tumor cell, this representation nicely controls for overall mRNA levels and reverse transcription efficiency, but more importantly, only represents KSHV-infected Kaposi's sarcoma cells not uninfected stromal cells. We discerned three groups of Kaposi's sarcoma tumors: Group I expressed only LANA and no K1; Group II tumors expressed both K1 and LANA but no Orf26; whereas Group III tumors expressed LANA, K1, and Orf26, indicative of lytic replication. These results correlate well with our K1 protein immunohistochemistry data shown in Fig. 6*A* and suggest that K1 is expressed to varying levels in most Kaposi's sarcoma tumors, and more importantly, that K1 can be expressed in the absence of late lytic replication. Indeed, we have observed that the K1 promoter is active in endothelial cells in the absence of the lytic transactivator Orf50/Rta (45). We speculate that it is in those endothelial cells that undergo abortive lytic replication, or that respond to certain environmental stimuli, that K1 displays its oncogenic potential.

Discussion

A novel finding of our report is that the KSHV K1 viral protein can immortalize primary human vein umbilical endothelial cells, a cell type relevant to KSHV biology. Prior studies on the transforming properties of K1 were restricted to rodent cells, which are much more susceptible to neoplasia and spontaneous transformation than human cells (46). We found that expression of K1 in primary HUVECs extended their life span significantly compared with the GFP-expressing control. Although these cells were immortalized, they were not transformed. Immortalization of HUVECs by K1 did not involve the up-regulation of telomerase activity, suggesting that telomere maintenance in K1-expressing HUVECs occurs via the ALT pathway (47).

Activation of the VEGF/VEGFR signaling pathway is critical to the survival of endothelial cells (48, 49), and here, we report that this pathway is highly up-regulated in K1-expressing endothelial cells. Moreover, PI3K/Akt, another key pathway mediating cell survival, is also activated in these cells. Interestingly, K1 expression in endothelial cells resulted in activation of PI3K, PDK1, and Akt and inactivation of PTEN. Activation of Akt kinase was mediated by PI3K because LY294002, a PI3K inhibitor, severely inhibited Akt activation. Moreover, all of the downstream targets of the PI3K/Akt pathway were phosphorylated in endothelial cells, including FKHR, Bad, GSK3β, and mTOR. This is in striking contrast to the scenario in B cells, where K1 expression specifically only affected the phosphorylation and inactivation of FKHR protein (15). This suggests that cell type differences between B cells and endothelial cells may alter the downstream effector molecules targeted by K1 and that the extended substrate range in endothelial cells resulted in the pro-growth phenotype reported herein. Alternatively, the SH2 binding motifs that comprise the K1 ITAM are more active in non-hematopoietic cells, similar to other ITAM signaling moieties (50). It was recently reported that mTOR is activated in Kaposi's sarcoma tumors, and that Sirolimus (rapamycin), an mTOR inhibitor, could induce Kaposi's sarcoma tumor regression (51). In this report, we have identified K1 as a viral protein responsible for activation of mTOR.

Recent data suggest that human cells require perturbation in at least six pathways to generate neoplastic transformation, and that activation of the PI3K pathway is critical for transformation of several different types of human cells (46). Thus, the activation of the PI3K/Akt pathway and inactivation of PTEN by K1 may be important for the initial development of KSHV-associated endothelial cell hyperplasia.

We also observed that K1 expression in already tumorigenic C33A cells further enhanced their tumorigenicity in nude mice, with the K1-expressing C33A tumors growing significantly faster and larger than the GFP vector–expressing tumors. The C33A-K1 tumors, like the HUVEC-K1 cells, displayed increased Akt phosphorylation and Ki67 expression. The K1-expressing C33A tumors also seemed more vascularized than the GFP-expressing C33A tumors.

KSHV K1 is expressed in PELs and MCD (42), and here, we show that K1 is also expressed in Kaposi's sarcoma lesions at both the mRNA and protein level (Fig. 6). Thus, our data suggest that K1 contributes to the initial and sustained immortalization of human endothelial cells, and K1's activation of the PI3K/Akt cell survival pathway likely constitutes the molecular mechanism for this phenotype. Our data also suggest a second role in that K1 augments angiogenesis of already established tumors, and we suggest a paracrine role for K1 whereby activation of the VEGF/VEGFR and PI3K pathway in endothelial cells contributes to viral-induced pathogenesis and KSHV-associated angiogenesis.

Acknowledgments

Received 10/11/2005; revised 1/13/2006; accepted 2/3/2006.

Grant support: AACR Gertrude B. Elion Cancer Research award (B. Damania) and NIH grants CA096500 (B. Damania), HL083469 (B. Damania), CA109232 (D.P. Dittmer), and CA110136 (D.P. Dittmer).

The costs of publication of this article were defrayed in part by the payment of page charges. This article must therefore be hereby marked *advertisement* in accordance with 18 U.S.C. Section 1734 solely to indicate this fact.

We thank Dr. Jae U. Jung (Department of Microbiology and Molecular Genetics and Tumor Virology Division, New England Primate Research Center, Harvard Medical School, Southborough, MA) for kindly providing us with the polyclonal anti-K1 antibody, Dr. E. Mesri (Laboratory of Viral Oncogenesis, Department of Medicine, Weill Medical College of Cornell University, New York, NY) for the pLXCN/GFP vector, the ACSR for Kaposi's sarcoma tumor microarray slides and banked specimens, and the members of the Damania and Dittmer labs for helpful discussions.

References

1. Chang Y, Cesarman E, Pessin MS, et al. Identification of herpesvirus-like DNA sequences in AIDS-associated Kaposi's sarcoma. Science 1994;266:1865–9.
2. Dupin N, Grandadam M, Calvez V, et al. Herpesvirus-like DNA sequences in patients with Mediterranean Kaposi's sarcoma. Lancet 1995;345:761–2.
3. Moore PS, Chang Y. Detection of herpesvirus-like DNA sequences in Kaposi's sarcoma in patients with and without HIV infection. N Engl J Med 1995;332:1181–5.
4. Cesarman E, Chang Y, Moore PS, Said JW, Knowles DM. Kaposi's sarcoma-associated herpesvirus-like DNA sequences in AIDS- related body-cavity-based lymphomas. N Engl J Med 1995;332:1186–91.
5. Soulier J, Grollet L, Oksenhendler E, et al. Kaposi's sarcoma-associated herpesvirus-like DNA sequences in multicentric Castleman's disease. Blood 1995;86:1276–80.
6. Boshoff C, Schulz TF, Kennedy MM, et al. Kaposi's sarcoma-associated herpesvirus infects endothelial and spindle cells. Nat Med 1995;1:1274–8.
7. Cornali E, Zietz C, Benelli R, et al. Vascular endothelial growth factor regulates angiogenesis and vascular permeability in Kaposi's sarcoma. Am J Pathol 1996;149:1851–69.
8. Staskus KA, Zhong W, Gebhard K, et al. Kaposi's sarcoma-associated herpesvirus gene expression in endothelial (spindle) tumor cells. J Virol 1997;71:715–9.
9. Cacciotti P, Libener R, Betta P, et al. SV40 replication in human mesothelial cells induces HGF/Met receptor activation: a model for viral-related carcinogenesis of human malignant mesothelioma. Proc Natl Acad Sci U S A 2001;98:12032–7.
10. Damania B. Gammaherpesviruses of non-human primates. In: Human herpesviruses: biology, therapy and immunoprophylaxis. Cambridge (UK): Cambridge University Press; 2004.
11. Lee H, Veazey R, Williams K, et al. Deregulation of cell growth by the K1 gene of Kaposi's sarcoma-associated herpesvirus. Nat Med 1998;4:435–40.
12. Prakash O, Swamy OR, Peng X, et al. Activation of Src kinase Lyn by the Kaposi sarcoma-associated herpes virus K1 protein: implications for lymphomagenesis. Blood 2005;105:3987–94.
13. Harvey DM, Levine AJ. p53 alteration is a common event in the spontaneous immortalization of primary BALB/c murine embryo fibroblasts. Genes Dev 1991;5:2375–85.
14. Lee H, Guo J, Li M, et al. Identification of an immunoreceptor tyrosine-based activation motif of K1 transforming protein of Kaposi's sarcoma-associated herpesvirus. Mol Cell Biol 1998;18:5219–28.
15. Tomlinson CC, Damania B. The K1 protein of Kaposi's sarcoma-associated herpesvirus activates the Akt signaling pathway. J Virol 2004;78:1918–27.
16. Wang L, Wakisaka N, Tomlinson CC, et al. The Kaposi's sarcoma-associated herpesvirus (KSHV/HHV8) K1 protein induces expression of angiogenic and invasion factors. Cancer Res 2004;64:2774–81.
17. Neufeld G, Cohen T, Gengrinovitch S, Poltorak Z. Vascular endothelial growth factor (VEGF) and its receptors. FASEB J 1999;13:9–22.
18. Cross MJ, Claesson-Welsh L. FGF and VEGF function in angiogenesis: signalling pathways, biological responses and therapeutic inhibition. Trends Pharmacol Sci 2001;22:201–7.
19. Carpenter CL, Cantley LC. Phosphoinositide 3-kinase and the regulation of cell growth. Biochim Biophys Acta 1996;1288:M11–6.
20. Dayanir V, Meyer RD, Lashkari K, Rahimi N. Identification of tyrosine residues in vascular endothelial growth factor receptor-2/FLK-1 involved in activation of phosphatidylinositol 3-kinase and cell proliferation. J Biol Chem 2001;276:17686–92.
21. Toker A. Protein kinases as mediators of phosphoinositide 3-kinase signaling. Mol Pharmacol 2000;57:652–8.
22. Anderson KE, Coadwell J, Stephens LR, Hawkins PT. Translocation of PDK-1 to the plasma membrane is important in allowing PDK-1 to activate protein kinase B. Curr Biol 1998;8:684–91.
23. Thompson JE, Thompson CB. Putting the rap on Akt. J Clin Oncol 2004;22:4217–26.
24. Yao L, Salvucci O, Cardones AR, et al. Selective expression of stromal-derived factor-1 in the capillary vascular endothelium plays a role in Kaposi's sarcoma pathogenesis. Blood 2003;102:3900–5.
25. Dudek H, Datta SR, Franke TF, et al. Regulation of neuronal survival by the serine-threonine protein kinase Akt. Science 1997;275:661–5.
26. Kennedy SG, Kandel ES, Cross TK, Hay N. Akt/Protein kinase B inhibits cell death by preventing the release of cytochrome *c* from mitochondria. Mol Cell Biol 1999;19:5800–10.
27. Datta SR, Dudek H, Tao X, et al. Akt phosphorylation of BAD couples survival signals to the cell-intrinsic death machinery. Cell 1997;91:231–41.
28. del Peso L, Gonzalez-Garcia M, Page C, Herrera R, Nunez G. Interleukin-3-induced phosphorylation of BAD through the protein kinase Akt. Science 1997;278:687–9.
29. Cross DA, Alessi DR, Cohen P, Andjelkovich M, Hemmings BA. Inhibition of glycogen synthase kinase-3 by insulin mediated by protein kinase B. Nature 1995;378:785–9.
30. Gingras AC, Kennedy SG, O'Leary MA, Sonenberg N, Hay N. 4E-BP1, a repressor of mRNA translation, is phosphorylated and inactivated by the Akt(PKB) signaling pathway. Genes Dev 1998;12:502–13.
31. Bais C, Van Geelen A, Eroles P, et al. Kaposi's sarcoma associated herpesvirus G protein-coupled receptor immortalizes human endothelial cells by activation of the VEGF receptor-2/KDR. Cancer Cell 2003;3:131–43.
32. Colgin LM, Reddel RR. Telomere maintenance mechanisms and cellular immortalization. Curr Opin Genet Dev 1999;9:97–103.
33. Bryan TM, Englezou A, Dalla-Pozza L, Dunham MA, Reddel RR. Evidence for an alternative mechanism for maintaining telomere length in human tumors and tumor-derived cell lines. Nat Med 1997;3:1271–4.
34. Perrem K, Colgin LM, Neumann AA, Yeager TR, Reddel RR. Coexistence of alternative lengthening of telomeres and telomerase in hTERT-transfected GM847 cells. Mol Cell Biol 2001;21:3862–75.
35. Staudt MR, Kanan Y, Jeong JH, Papin JF, Hines-Boykin R, Dittmer DP. The tumor microenvironment controls primary effusion lymphoma growth *in vivo*. Cancer Res 2004;64:4790–9.
36. Gerber HP, McMurtrey A, Kowalski J, et al. Vascular endothelial growth factor regulates endothelial cell survival through the phosphatidylinositol 3′-kinase/Akt signal transduction pathway. Requirement for Flk-1/KDR activation. J Biol Chem 1998;273:30336–43.
37. Brunet A, Bonni A, Zigmond MJ, et al. Akt promotes cell survival by phosphorylating and inhibiting a Forkhead transcription factor. Cell 1999;96:857–68.
38. Scott PH, Brunn GJ, Kohn AD, Roth RA, Lawrence JC, Jr. Evidence of insulin-stimulated phosphorylation and activation of the mammalian target of rapamycin mediated by a protein kinase B signaling pathway. Proc Natl Acad Sci U S A 1998;95:7772–7.
39. Zong JC, Ciufo DM, Alcendor DJ, et al. High-level variability in the ORF-K1 membrane protein gene at the left end of the Kaposi's sarcoma-associated herpesvirus genome defines four major virus subtypes and multiple variants or clades in different human populations. J Virol 1999;73:4156–70.
40. Rincon-Arano H, Rosales R, Mora N, Rodriguez-Castaneda A, Rosales C. R-Ras promotes tumor growth of cervical epithelial cells. Cancer 2003;97:575–85.
41. Samaniego F, Pati S, Karp J, Prakash O, Bose D. Human herpesvirus 8 k1-associated nuclear factor-kappa b-dependent promoter activity: role in Kaposi's

sarcoma inflammation? J Natl Cancer Inst Monogr 2001;28:15–23.
42. Lee BS, Connole M, Tang Z, Harris NL, Jung JU. Structural analysis of the Kaposi's sarcoma-associated herpesvirus K1 protein. J Virol 2003;77:8072–86.
43. Fakhari FD, Dittmer DP. Charting latency transcripts in Kaposi's sarcoma-associated herpesvirus by whole-genome real-time quantitative reverse transcription-PCR. J Virol 2002;76:6213–23.
44. Dittmer DP. Transcription profile of Kaposi's sarcoma-associated herpesvirus in primary Kaposi's sarcoma lesions as determined by real-time PCR arrays. Cancer Res 2003;63:2010–5.
45. Bowser BS, DeWire SM, Damania B. Transcriptional regulation of the K1 gene product of Kaposi's sarcoma-associated herpesvirus. J Virol 2002;76:12574–83.
46. Rangarajan A, Hong SJ, Gifford A, Weinberg RA. Species- and cell type-specific requirements for cellular transformation. Cancer Cell 2004;6:171–83.
47. Grobelny JV, Kulp-McEliece M, Broccoli D. Effects of reconstitution of telomerase activity on telomere maintenance by the alternative lengthening of telomeres (ALT) pathway. Hum Mol Genet 2001;10:1953–61.
48. Nor JE, Christensen J, Mooney DJ, Polverini PJ. Vascular endothelial growth factor (VEGF)-mediated angiogenesis is associated with enhanced endothelial cell survival and induction of Bcl-2 expression. Am J Pathol 1999;154:375–84.
49. Reinmuth N, Liu W, Jung YD, et al. Induction of VEGF in perivascular cells defines a potential paracrine mechanism for endothelial cell survival. FASEB J 2001; 15:1239–41.
50. Katz E, Lareef MH, Rassa JC, et al. MMTV Env encodes an ITAM responsible for transformation of mammary epithelial cells in three-dimensional culture. J Exp Med 2005;201:431–9.
51. Stallone G, Schena A, Infante B, et al. for Kaposi's sarcoma in renal-transplant recipients. N Engl J Med 2005;352:1317–23.